Chiral Metal Gallophosphates Templated by Achiral Triamine: Syntheses and Characterizations of $A[Mn(H_2O)_2Ga(PO_4)_2]_3$ and $A[Zn_3Ga(PO_4)_4]\cdot H_2O$ (A = H_3DETA)

Chia-Her Lin and Sue-Lein Wang*

Department of Chemistry, National Tsing Hua University, Hsinchu 300, Taiwan

Received April 24, 2001. Revised Manuscript Received September 4, 2001

Two new transition-metal gallophosphates, $(H_3DETA)[Mn(H_2O)_2Ga(PO_4)_2]_3$ (**1**) and $(H_3DETA)[Zn_3Ga(PO_4)_4]\cdot H_2O$ (**2**) (DETA = $NH_2(CH_2)_2NH(CH_2)_2NH_2$), have been synthesized under mild hydrothermal conditions and characterized by single-crystal X-ray diffraction, thermogravimetric analysis, and magnetic susceptibility data. They are the first transition-metal gallophosphates that adopt chiral frameworks with achiral triamine templates. Both can be prepared in pure chiral forms. The structure of **1** consists of octahedra of $MnO_4(H_2O)_2$ and tetrahedra of GaO_4 and PO_4 to form a three-dimensional 4-connected polyhedral network in CZP topology. The most interesting feature lies in the fact that the structure is well-sustained with all water ligands removed from the octahedral Mn^{2+} centers. The dehydration−hydration process for the coordination water is reversible. On the basis of TG analysis, material **1** can be thermally stable up to ≈300 °C. Material **2** is built up with tetrahedra of MO_4 (M = Zn and Ga) and PO_4 and crystallizes in the UCSB-7 structure type. It has the highest transition-metal-to-gallium ratio among MGaPOs. Crystal data: **1**, orthorhombic, $C222_1$, a = 10.0390(6) Å, b = 17.389(1) Å, c = 16.7356(9) Å, Z = 4; **2**, cubic, $I4_132$, a = 17.9192(6) Å, Z = 12.

Introduction

The synthesis of open-framework metal phosphates, in particular those of aluminum and gallium, has attracted much attention for their rich structural chemistry, zeolitic property, and potential applications as molecular sieves, catalysts, and ion exchangers.[1−5] The physical and chemical properties of these materials can be modified or manipulated by incorporating heteroatoms into the existing AlPO and GaPO frameworks to form $M_xAl_{1-x}PO$s and $M_xGa_{1-x}PO$s.[6−9] The presence of transition-metal (M) ions during synthesis can also lead to novel open frameworks, more likely of MGaPOs due to the propensity of gallium to adopt a more variable and expanded coordination environment compared to aluminum. Recently, we started investigations in direct synthesis of novel MGaPO structures employing dibasic amines as templates via mild hydrothermal routes. This had resulted in several unique MGaPO (M = Mn, Zn, V) structures templated by diprotonated diamine molecules.[10−13] Since the discovery of the first 24R-channel gallophosphate, NTHU-1,[14] prepared from diethylenetriamine (DETA), we have continued to pursue the synthesis of microporous MGaPOs using such a tribasic amine as the structure-directing agent. To the best of our knowledge, neither MGaPOs nor GaPOs encapsulating triple-charged amine cations were previously documented. Our approach has successfully yielded the first chiral MnGaPO, $(H_3DETA)[Mn(H_2O)_2Ga(PO_4)_2]_3$ (**1**), which consists of octahedra of $MnO_4(H_2O)2$ and tetrahedra of GaO_4 and PO_4, and can be thermally stable up to ≈300 °C. Upon heating to 250 °C, all water ligands on the octahedral Mn^{2+} ions can be removed while the structure remains intact. The dehydrated form then contains tetrahedral Mn^{2+} centers, which will resume six coordination by retrieving water molecules from humidity. As zinc ions can be more stable in tetrahedral coordination, we have proceeded to synthesize the zinc analogue of the dehydrated form of **1**. When Mn^{2+} ions are replaced with Zn^{2+} ions, the reaction yields the first chiral ZnGaPO material, $(H_3DETA)[Zn_3Ga(PO_4)_4]\cdot H_2O$ (**2**), which unexpectedly adopts a different framework topology from **1**. Both of them can be prepared in pure chiral forms. *Herein* the hydrothermal syntheses, crystal structures (including the dehydrated

* To whom correspondence should be addressed. E-mail: slwang@mx.nthu.edu.tw. Fax: 886-35711082. Tel.: 886-35721074.

(1) Xiao, F. S.; Qiu, S.; Pang, Q. W.; Xu, R. *Adv. Mater.* **1999**, *11*, 1091.
(2) Cheetham, A. K.; Ferey, G.; Loiseau, T. *Angew. Chem., Int. Ed.* **1999**, *38*, 3268.
(3) Davis, M. E. *Microporous Mesoporous Mater.* **1998**, *21*, 173.
(4) Thomas, J. M. *Angew Chem., Int. Ed. Engl.* **1988**, *27*, 1673; *Angew Chem., Int. Ed.* **1999**, *38*, 3588.
(5) Ying, J. Y.; Wong, M. S. *Angew. Chem., Int. Ed.* **1999**, *38*, 56.
(6) Bu, X.; Feng, P.; Stucky, G. D. *Science* **1997**, *278*, 2080.
(7) Chippindale, A. M.; Cowley, A. R. *Microporous Mesoporous Mater.* **1998**, *21*, 271.
(8) Hartmann, M.; Kevan, L. *Chem. Rev.* **1999**, *99*, 635.
(9) Feng, P.; Bu, X.; Stucky, G. D. *Nature* **1997**, *388*, 735.
(10) Hsu, K. F.; Wang, S. L. *Chem. Commun.* **2000**, 135.
(11) Lin, C. H.; Wang, S. L. *Chem. Mater.* **2000**, *12*, 3617.
(12) Hsu, K. F.; Wang, S. L. *Inorg. Chem.* **2000**, *39*, 1773.
(13) Three novel VGaPOs prepared by Huang, L. H.; Wang, S. L, to be submitted.
(14) Lin, C. H.; Wang, S. L.; Lii, K. H. *J. Am. Chem. Soc.* **2001**, *123*, 4649.

10.1021/cm010421v CCC: $22.00
Published on Web 12/20/2001

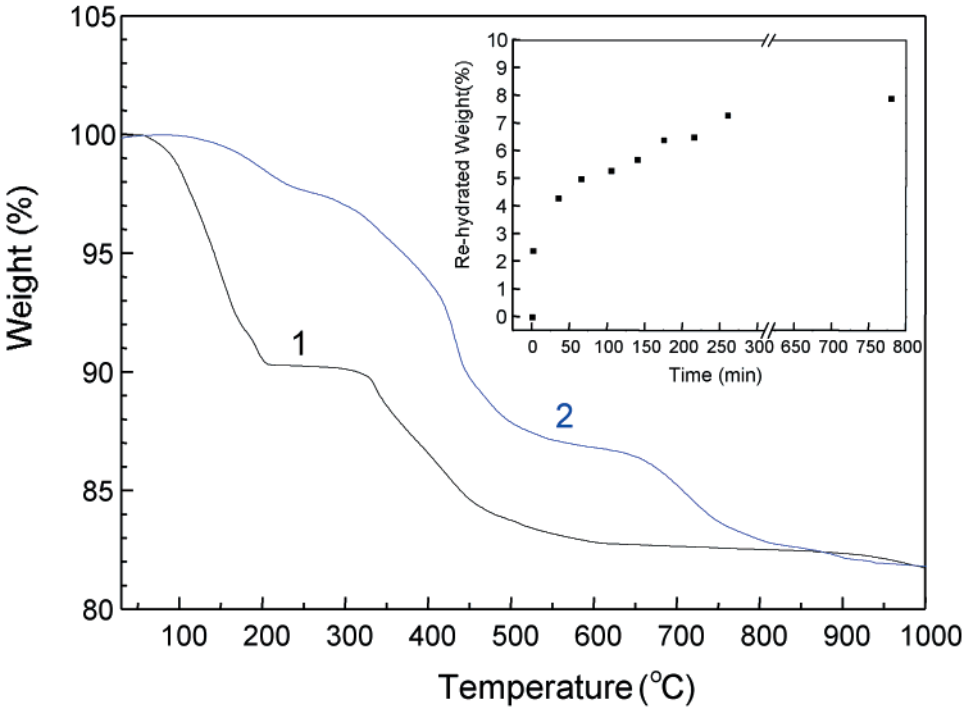

Figure 1. TGA curves for $(H_3DETA)[Mn(H_2O)_2Ga(PO_4)_2]_3$ (**1**) and $(H_3DETA)[Zn_3Ga(PO_4)_4]\cdot H_2O$ (**2**) in flowing N_2 at 10 °C min^{-1}. The rehydration rate of a dehydrated powder sample is shown in the inset (see text for detail).

form of **1**), and thermal analyses on both **1** and **2** and the magnetic study of **1** are presented and discussed.

Experimental Section

Syntheses and Compositional Characterization. Chemicals of reagent grade or better were used as-received and all reactions were carried out in Teflon-lined digestion bombs (internal volume of 23 mL) under autogenous pressure by heating the reaction mixtures at either 160 or 180 °C for 3 days followed by slow cooling at 6 °C h^{-1} to room temperature. Crystals of **1** were initially obtained as a minor phase from the reaction used to prepare the mixed-valence compound of $(C_4H_{10}N_2)_2Mn^{II}Mn^{III}Ga_5(H_2O)(PO_4)_8$,[10] but with piperazine replaced by DETA. An optimum condition was achieved by heating $Ga(NO_3)_3\cdot xH_2O$ (1.2 mmol), $MnCl_2\cdot 2H_2O$ (1.2 mmol), 85% H_3PO_4 (6.0 mmol), DETA (3.45 mmol) in the solution of ethyleneglycol (6.0 mL), and H_2O (6.0 mL) (initial pH ~5.0). The product was nearly a single phase of **1**. As the reactant $MnCl_2\cdot 2H_2O$ was replaced by an equivalent amount of $ZnCl_2$, the reaction yielded crystals of **2**. Powder XRD measurements were performed on picked crystals to confirm the phase purity before all chemical and physical analyses. Elemental analyses were carried out to confirm the organic contents. Anal. Found/calcd for **1**: C, 4.21/4.15; N, 3.58/3.65; H, 2.41/2.44%. Anal. Found/calcd for **2**: C, 5.90/6.23; N, 4.98/5.46; H, 2.18/2.33%. For both compounds, the M-to-Ga ratio determined from single-crystal structure analyses (vide infra) were further confirmed by electron probe microanalysis (EPMA) data.

Thermal Study. Thermogravimetric analyses (TGA), using a Seiko TG 300 analyzer, were performed on powder samples of **1** (8.52 mg) and **2** (8.71 mg) under flowing N_2 with a heating rate of 10 °C min^{-1}. For **1**, two stages of weight loss over the range 40−210 and 310−650 °C were observed (Figure 1). The first stage should be attributed to the removal of coordination waters on the Mn^{2+} ions (calcd 9.33% for 6 H_2O per formula unit). The second stage should correspond to the removal of the organic content and further dehydration (calcd 8.89% for 1 mol of DETA and 2.33% for 1.5 H_2O). The total observed weight loss (19.7%) for the two stages can be compared with the calculated weight loss (20.55%) based on the above interpretation. The thermal stability of the structure of **1** was further confirmed by heating 105.0 mg powders of **1** at 250 °C for 16 h. Immediate weighing of the final product of the thermal treatment revealed a 9.3% of mass loss, corresponding to all six coordination waters per formula unit. The dehydrated reabsorbed water rapidly (see the inset in Figure 1) and the dehydration−hydration process is reversible. Single crystals of **1** were treated at 250 °C (under 1 atm of air) for 5 h and the structure was analyzed again. As indicated by the results from both powder and single-crystal studies, the structure of **1** is well-sustained after heating.

The TG curve of **2** showed unresolved three stages of weight losses. The first stage (100 to ca. 220 °C) corresponds to the release of lattice water. The second and third stages should correspond to the decomposition of DETA molecules and removal of retained carbon. After heating to 1000 °C, the solid residue looked gray and was X-ray amorphous. The total observed weight loss (18.3%) is close to the expected weight loss (19.23% for 1 DETA and 2.5 H_2O). The reduction in observed mass loss is likely due to incomplete removal of the carbon residue.

Single-Crystal Structure Analysis. Crystals of dimensions 0.20 × 0.20 × 0.40 mm for **1** and 0.40 × 0.40 × 0.40 mm for **2** were selected for indexing and intensity data collection. The diffraction measurements were performed on Bruker *Smart*-CCD diffractometers (λ = 0.71073 Å). Intensity data were collected in 1271 frames with increasing ω (0.3° per frame) and corrected for *Lp* and absorption effects using the *SADABS* program.[15] Number of measured and unique reflections with $I > 2\sigma_I$: 7430 (14134) and 3396 (1060) for **1** (**2**). The intensity data of **1** were first averaged in the Laue group $6/mmm$ (R_{int} = 3.31%) and the space group $P6_122$ (or $P6_522$) was assigned. All framework atoms of Ga, Mn, P, and O but no rational fragments of organic cations could be located on electron-density maps. After many trials and further scrutiny in the symmetry, the intensity data were finally averaged in the $2/mmm$ Laue group (R_{int} = 2.95%) and the space group $C222_1$ was reassigned. The moiety of the DETA molecule was then clearly observed in the Fourier difference map. For compound **2**, intensity data were averaged in the Laue group 432 (R_{int} = 3.12%) and the structure well-refined in the space group $I4_132$. The amine cations severely disordered and barely

(15) Sheldrick, G. M. *SADABS*; Siemens Analytical X-ray Instrument Division: Madison, WI, 1998.

Table 1. Crystallographic Data for 1, Dehydrated 1, and 2

	1	**1** (dehydrated)	**2**
formula	$C_4H_{28}Ga_3Mn_3N_3O_{30}P_6$	$C_4H_{22}Ga_3Mn_3N_3O_{27}P_6$	$C_4H_{18}GaN_3O_{17}P_4Zn_3$
fw	1158.1	1104.1	769.98
space group	$C222_1$	$C222_1$	$I4_132$
a, Å	10.0390(6)	10.039(2)	17.9192(6)
b, Å	17.3885(10)	17.401(3)	
c, Å	16.7356(9)	16.503(3)	
volume, Å^3	2921.4(3)	2882.8(8)	5753.8(9)
Z	4	4	12
D_{cacl}, g cm^{-3}	2.633	2.668	2.666
μ, mm^{-1}	4.439	4.498	5.524
T, °C	22	22	22
λ, Å	0.71073	0.71073	0.71073
R1[a]	0.0390	0.0688	0.0347
wR2[b]	0.0971	0.1896	0.1222

[a] $R1 = \sum||F_o| - |F_c||/\sum|F_o|$ for $F_o > 4\sigma(F_o)$. [b] $wR2 = [\sum w(|F_o|^2 - |F_c|^2)^2]/\sum w(|F_o|^2)^2]^{1/2}$ for all data, where $w = [\sigma^2(F_o^2) + 0.0427P]2 + 19.07P]$ for **1** and $w = [\sigma^2(F_o^2) + 0.0861P]^2 + 0.35P]$ for **2**.

Table 2. Atomic Coordinates ($\times 10^4$) and Thermal Parameters (Å$^2 \times 10^3$) for 1 and 2

atom	x	y	z	U_{eq}[a]
		1		
Ga(1)	5000	6571(1)	7500	14(1)
Ga(2)	2647(1)	5785(1)	9167(1)	14(1)
Mn(1)	10000	4592(1)	7500	21(1)
Mn(2)	3113(1)	2297(1)	9167(1)	21(1)
P(1)	4799(1)	6994(1)	9242(1)	15(1)
P(2)	1908(1)	4104(1)	9093(1)	15(1)
P(3)	7890(1)	6098(1)	7577(1)	15(1)
O(1)	4345(4)	6131(3)	9252(3)	23(1)
O(2)	4837(4)	7234(2)	8343(2)	19(1)
O(3)	6188(4)	7023(3)	9598(3)	25(1)
O(4)	3791(5)	7497(3)	9656(3)	29(1)
O(5)	2970(4)	4759(2)	9082(3)	23(1)
O(6)	1569(4)	3967(3)	9989(2)	18(1)
O(7)	2561(5)	3400(2)	8732(3)	25(1)
O(8)	659(5)	4360(3)	8680(3)	28(1)
O(9)	6375(4)	5893(2)	7593(3)	22(1)
O(10)	8271(4)	6197(3)	6676(2)	20(1)
O(11)	8620(5)	5415(3)	7927(3)	24(1)
O(12)	8136(5)	6855(3)	7982(3)	29(1)
O(13)	8567(8)	3573(3)	7790(4)	53(2)
O(14)	5356(6)	2500(4)	8873(4)	57(2)
O(15)	3920(6)	1096(4)	9470(3)	55(2)
N(1)	7316(6)	4263(4)	9167(3)	400(30)
N(2)	5000(6)	3472(4)	7499(3)	230(20)
C(1)	6016(6)	4135(4)	8708(3)	224(18)
C(2)	5705(6)	4102(4)	7981(3)	200(15)
		2		
M(1)[b]	973(1)	4921(1)	3611(1)	19(1)
P(1)	1518(1)	6151(1)	2569(1)	19(1)
O(1)	43(2)	4468(2)	3794(2)	32(1)
O(2)	1418(2)	5246(2)	4498(2)	30(1)
O(3)	1641(2)	4226(2)	3188(2)	27(1)
O(4)	875(2)	5765(2)	2980(2)	27(1)

[a] U_{eq} is defined as one-third of the trace of the orthogonallized U_{ij} tensor. [b] The M(1) atom site is occupied by both gallium (25%) and zinc (75%) atoms.

Table 3. Selected Bond Lengths (Å) and Bond Valence Sums ($\sum S$) for 1 and 2

		1	
Ga(1)−O(2)	1.830(4)	Ga(1)−O(2)[a]	1.830(4)
Ga(1)−O(9)	1.821(4)	Ga(1)−O(9)[a]	1.821(4)
$\sum S$[Ga(1)−O] = 3.09			
Ga(2)−O(1)	1.813(4)	Ga(2)−O(5)	1.819(4)
Ga(2)−O(6)[b]	1.831(4)	Ga(2)−O(10)[b]	1.832(4)
$\sum S$[Ga(2)−O] = 3.11			
Mn(1)−O(8)[a]	2.122(4)	Mn(1)−O(8)[d]	2.122(4)
Mn(1)−O(11)	2.115(5)	Mn(1)−O(11)[c]	2.115(5)
Mn(1)−O(13)	2.334(7)	Mn(1)−O(13)[c]	2.334(7)
$\sum S$[Mn(1)−O] = 2.11			
Mn(2)−O(3)[e]	2.117(5)	Mn(2)−O(4)[b]	2.115(5)
Mn(2)−O(7)	2.124(4)	Mn(2)−O(12)[e]	2.127(4)
Mn(2)−O(14)	2.298(7)	Mn(2)−O(15)	2.332(7)
$\sum S$[Mn(2)−O] = 2.12			
P(1)−O(1)	1.568(4)	P(1)−O(2)	1.562(4)
P(1)−O(3)	1.517(5)	P(1)−O(4)	1.506(5)
$\sum S$[P(1)−O] = 4.97			
P(2)−O(5)	1.560(4)	P(2)−O(6)	1.556(4)
P(2)−O(7)	1.515(4)	P(2)−O(8)	1.499(5)
$\sum S$[P(2)−O] = 5.04			
P(3)−O(9)	1.562(4)	P(3)−O(10)	1.564(4)
P(3)−O(11)	1.513(5)	P(3)−O(11)	1.502(5)
$\sum S$[P(3)−O] = 5.00			
N(1)−C(1)	1.530(8)	N(2)−C(2)	1.533(8)
N(2)−C(2)[a]	1.533(8)	C(1)−C(2)	1.257(8)
		2	
M(1)−O(1)	1.882(4)	M(1)−O(2)	1.873(4)
M(1)−O(3)	1.885(4)	M(1)−O(4)	1.896(3)
$\sum S$[Ga(1)−O] = 2.63		$\sum S$[Zn(1)−O] = 2.45	
P(1)−O(1)[f]	1.531(4)	P(1)−O(2)[g]	1.535(4)
P(1)−O(3)[h]	1.532(4)	P(1)−O(4)	1.531(4)
$\sum S$[P(1)−O] = 5.03			

[a] Symmetry codes: $-x + 1, y, -z + 3/2$. [b] $x, -y + 1, -z + 2$. [c] $-x + 2, y, -z + 3/2$. [d] $x + 1, y, z$. [e] $x - 1/2, y - 1/2, z$. [f] $z - 1/4, y + 1/4, -x + 1/4$. [g] $-y + 3/4, -x + 3/4, -z + 3/4$. [h] $x + 0, -y + 1, -z + 1/2$.

no organic moiety could be located. A lower symmetry space group $I2_13$ was tried but without significant improvement. Both structures were solved by direct methods. Structural parameters were refined based on F^2. The final cycle of refinements, including the atomic coordinates and anisotropic thermal parameters for all non-hydrogen atoms, converged at $R = 0.0390$ (0.0347) for **1** (**2**). The refined Flack parameter is 0.03(2) for **1** and −0.02(3) for **2**. All calculations were performed by using *SHELXTL* programs.[16] Crystallographic data are given in Table 1. Atomic coordinates and thermal parameters are in Table 2 and selected bond distances in Table 3. Other details for the refinement are given in the Supporting Information.

Magnetic Susceptibility Measurements. A 150.0 mg powder sample of **1** was used to collect variable temperature magnetic susceptibility $\chi(T)$ data from 2 to 300 K in a magnetic field of 0.5 T using a Quantum Design SQUID magnetometer. The measured susceptibility data were corrected for core diamagnetism.[17] The effective magnetic moment (μ_{eff}) derived from the fit to Curie−Weiss law is close to the spin-only value, 5.82 vs 5.92 μB, indicating the manganese are present as high-

(16) Sheldrick, G. M. *SHELXTL programs*, Release Version 5.1; Bruker AXS, Madison, WI, 1998.

(17) Selwood, P. W. *Magnetochemistry*; Interscience: New York, 1956.

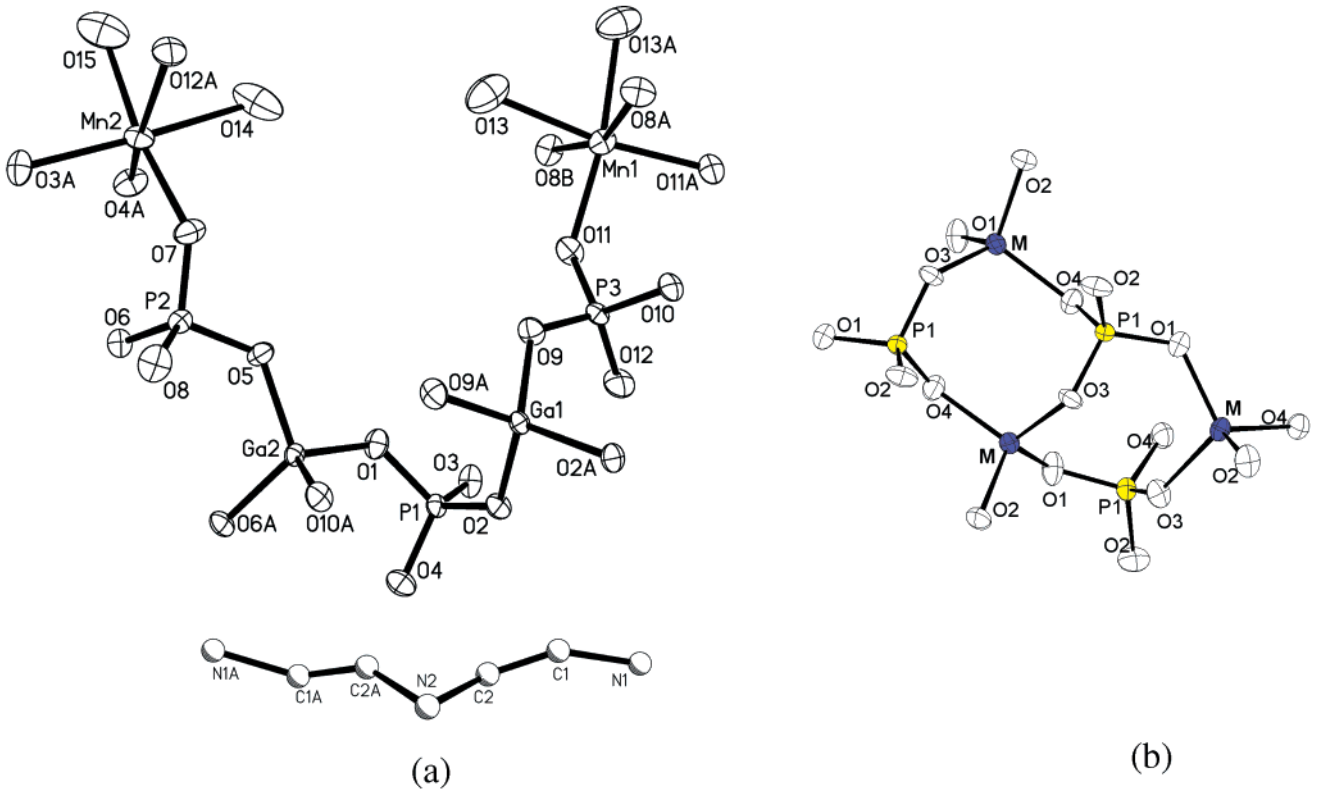

Figure 2. ORTEP of the asymmetric unit of **1** (left) and **2** (right), showing the labeling scheme and the local coordination. Thermal ellipsoids are shown at 50% probability.

spin Mn^{2+}. The small reduction in the observed μ_{eff} is due to weak antiferromagnetism as disclosed by the decreasing $\chi_M T$ value at low temperature and the negative sign of the Weiss constant (−1.3 K).

Results and Discussion

The asymmetric unit of **1**, as depicted in Figure 2, consists of two unique octahedral Mn^{2+} sites, two unique tetrahedral Ga^{3+} sites, and three unique tetrahedral P^{5+} sites. All atoms are residing on general positions except Mn(1) and Ga(1), which are located on 2-fold axes along *b*. The seven unique polyhedral centers form two kinds of 4-rings, one contains four tetrahedra ($2GaO_4 + 2PO_4$) and other contains one octahedron ($MnO_4(H_2O)_2$) and three tetrahedra ($1GaO_4 + 2PO_4$). As shown in Figure 3, 4-rings of the former type interlink into $Ga(PO_4)_2$ ribbons by sharing trans corners. The ribbons are cross-linked further by $MnO_4(H_2O)_2$ to generate a mixed-polyhedron helical network in which two types of channels (A and B) are observed. Alternatively, the structure may be viewed as built up with $Mn(H_2O)_2Ga(PO_4)_2$ helices that interlink through the Mn(1) octahedra to form the 3D structure. The helical channel A, which is encircled by $Ga(PO_4)_2$ ribbons, is large enough to accommodate two arrays of triprotonated DETA molecules. The $Mn(H_2O)_2Ga(PO_4)_2$ helix enclosed the smaller channel B to where the water ligands are pointing. Without Ga atoms, the $Mn(H_2O)_2(PO_4)_2$ helices can still be weaved into a 3D framework in which 12-R helical ribbons exist (Figure 4). It is interesting to note all water ligands in the Mn octahedra can be removed without destroying the structure. On the basis of the result of a combined thermal and powder X-ray diffraction study, the dehydrated should contain tetrahedral $MnGa(PO_4)_2$ helices where the Mn^{2+} ions can resume octahedral coordination by retrieving water molecules from humidity (Figure 5). Single-crystal structure analysis on a heated crystal reveals all three O_w sites can be partially restored up to ≈50% occupancy (after exposure to air for several hours at ambient temperature). In such a dehydrated crystal, the Mn−O_w bonds become longer and the polyhedra of Mn and Ga more distorted.

To date, only five MnGaPO materials[10,11,18−21] were structurally characterized and reported. They are all achiral materials. Among them, four contain anionic frameworks in which Mn atoms occupy intraframework sites, and one contains a neutral framework in which Mn atoms occupy extraframework sites. As the sixth member in the MnGaPO system (Table 4), material **1** is worth noting for its chiral nature and highly negative-charged CZP framework topology. In the literature, three inorganic compounds, $Na_6[Co_{0.2}Zn_{0.8}PO_4]_6 \cdot 9H_2O$,[22] $NaZnPO_4 \cdot H_2O$,[23] and $Fe(H_2O)_2BP_2O_8 \cdot H_2O$,[24] were previously reported to adopt CZP topology. As a common feature, they contain lattice water molecules as an indispensable part to sustain the 3D framework. For example, complete removal of the lattice waters from $Na_6[Co_{0.2}Zn_{0.8}PO_4]_6 \cdot 9H_2O$ or $NaZnPO_4 \cdot H_2O$ will irreversibly result in unknown crystalline phases. Further-

(18) Bond, A. D.; Chippindale, A. M.; Cowley, A. R. *Zeolites* **1997**, *19*, 326.
(19) Chippindale, A. M.; Bond, A. D.; Cowley, A. R. *Chem. Mater.* **1997**, *9*, 2830.
(20) Chippindale, A. M.; Cowley, A. R.; Bond, A. D. *Acta Crystallogr., Sect. C* **1998**, *54*, 1.
(21) Overweg, A. R.; de Haan, J. W.; Magusin, P. C. M. M.; van Santen, R. A.; Sankar, G.; Thomas, J. M. *Chem. Mater.* **1999**, *11*, 1680.
(22) Rajic, N.; Logar, N. Z.; Kaucic, V. *Zeolites* **1997**, *15*, 672.
(23) Harrison, W. T. A.; Gier, T. E.; Stucky, G. D.; Broach, R. W.; Bedard, R. A. *Chem. Mater.* **1996**, *8*, 145.
(24) Yilmaz, A.; Bu, X.; Kiziyalli, M.; Stucky, G. D. *Chem. Mater.* **2000**, *12*, 3243.

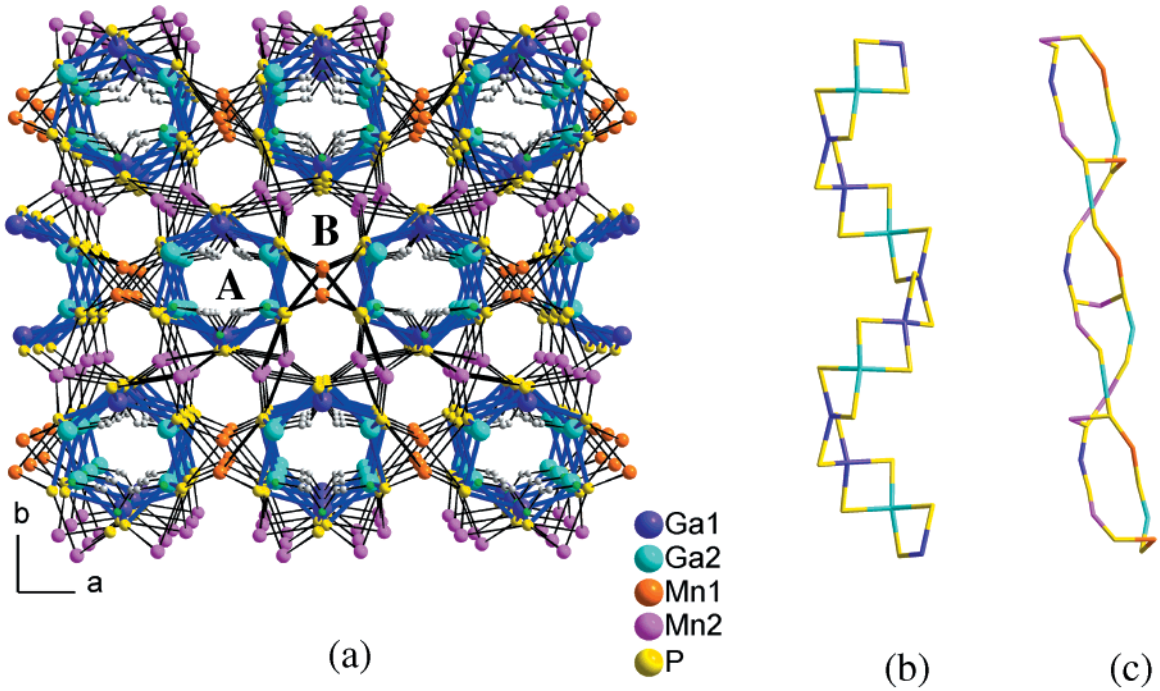

Figure 3. Helical structure of **1**. (a) Projection along *c* showing two kinds of straight tunnels A and B; (b) side view of the $Ga(PO_4)_2$ helix enclosing the tunnel A in which two arrays of H_3DETA^{3+} cations (carbon atoms in gray) are residing; (c) side view of the $Mn(H_2O)_2Ga(PO_4)_2$ helix enclosing the tunnel B.

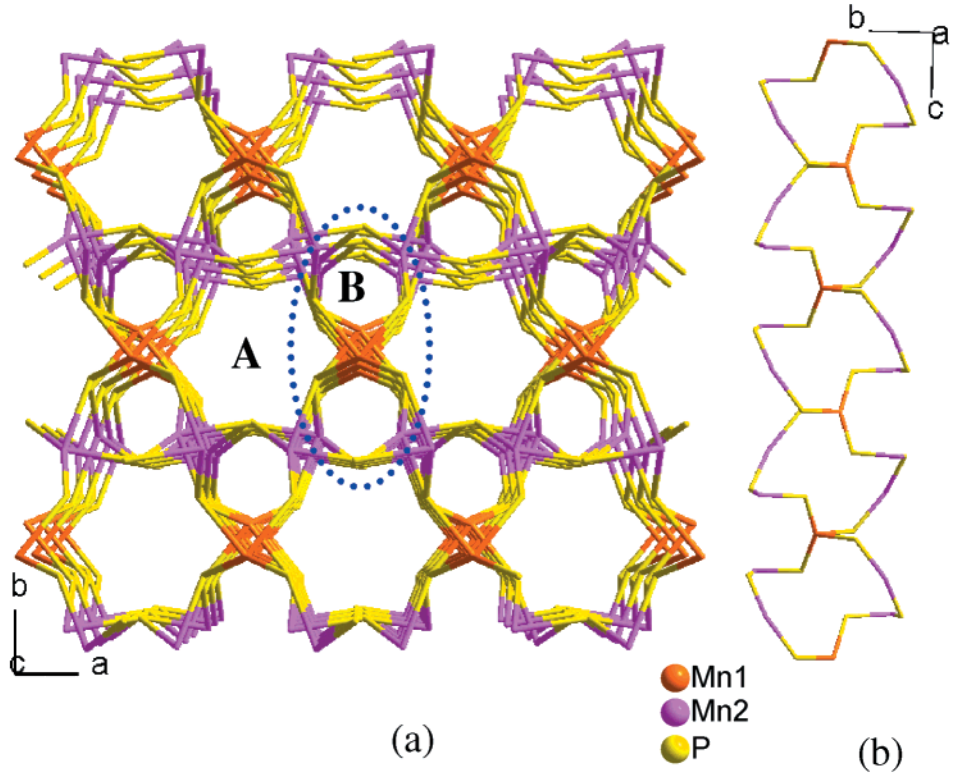

Figure 4. Helical framework (left) built up with $Mn(H_2O)_2(PO_4)_2$ helices (right), which contain 12-membered rings.

more, the removal of coordination waters from $Fe(H_2O)_2$-$BP_2O_8{\cdot}H_2O$ will collapse the structure and result in an amorphous nature. Compared with the three inorganic compounds, the amine-containing **1** is surprisingly the most stable with respect to heat. The reversible dehydration−hydration nature of the coordination waters on the Mn^{2+} ions is as well highly interesting. On the other hand, material **1** has a lower symmetry than the other three and is the only one that contains no lattice water. These are presumably due to the presence of unsymmetrical and large H_3DETA^{3+}cations in the channels where the lattice waters find no space to reside. Comparisons among the four CZP structures are summarized in Table 5.

Similarly, material **2** is the first chiral ZnGaPO material that adds one more structure type to the ZnGaPO system[24−27] (Table 4). In fact, it has the highest transition-metal-to-gallium ratio among all existing

Table 4. Summary of Structure Type, Atomic Ratio, Template, and Framework Composition for (a) MnGaPOs and (b) ZnGaPOs

(a)

	structure type	Mn:Ga:P	template	framework composition	refs
1	LAU	1:2:3	$[C_3H_5N_2]^+$	$[MnGa_2(PO_4)_3]^-$	18
2	new	1:1:3	$[C_6H_{14}N_2]^{2+}$	$[MnGa(HPO_4)_2(PO_4)]^{2-}$	19
3	*a*	1:2:3	NH_4^+	$[Mn(H_2O)_2Ga_2(PO_4)_3]^-$	20, 21
4	new	2:5:8	$(C_4H_{12}N_2)^{2+}$	$[Mn_2Ga_5(H_2O)(PO_4)_8]^{2-}$	10
5	new	3:4:6	none	$[Mn_3(H_2O)_6Ga_4(PO_4)_6]$	12
6	CZP	**1:1:2**	$[H_3DETA]^{3+}$	$[Mn_3(H_2O)_6Ga_3(PO_4)_6]^{3-}$	this work, **1**

(b)

	structure type	Zn:Ga:P	template	framework composition	refs
1	SOD	1:1:1	$[H_2NC_7H_{14}NH_3]^+$	$[Zn_xGa_{1-x}PO_4]^-$ (UCSB-6)	6
	SOD	1:2:3	$[C_4H_{12}N]^+$	$[ZnGa_2P_3O_{12}]^-$	7
2	LAU	1:2:3	$[C_5H_6N]^+$	$[ZnGa_2P_3O_{12}]^-$	7
3	GIS	1:1:2	$[H_2NC_7H_{14}NH_3]^+$	$[ZnGaP_2O_8]^-$ (UCSB-10);	6
	GIS	1:1:2	$[CN_3H_6]^+$; $[C_4NH_{10}]^+$	$[ZnGaP_2O_8]^-$	25
4	*a*	1:2:3	NH_4^+	$[ZnGa_2P_3O_{12}(H_2O)_2]^-$	21
5	CGS	1:3:4	$[C_7H_{14}N]^+$	$[ZnGa_3P_4O_{16}]^-$ (ZnGaPO-6)	25
	CGS	1:1:2	$[H_2DACH]^{2+}$	$[Zn_2Ga_2(PO_4)_4]^{2-}$	11
6	ZGP[b]	4:2:7	$[H_2DACH]^{2+}$	$[Zn_4Ga_2(HPO_4)_3(PO_4)_4]^{2-}$	11
7	Analcime	2:1:3	$(NH_4)_2^{2+}$	$[Zn_2GaP_3O_{12}]^{2-}$	26
8	Paracelsian	1:1:2	NH_4^+	$[ZnGaP_2O_8]^-$	26
9	UCSB-7	**3:1:4**	$[H_3DETA]^{3+}$	$[Zn_3Ga(PO_4)_4]^{3-}$	this work, **2**

[a] Isostructural with $NH_4[CoGa_2P_3O_{12}(H_2O)_2]$.[27] [b] New structure type code proposed to IZA.

Table 5. Summary of Cations, Framework Composition, Space Groups, and Cell Dimensions for the Materials Adopting CZP Framework Topology

cation	framework	lattice water	space group	*a*/Å	*b*/Å	*c*/Å	*V*/Å	refs
Na^+	$[Co_{0.2}Zn_{0.8}PO_4]^-$	1.5 H_2O	$P6_1$	10.48	10.480	15.09	1435	20
Na^+	$[ZnPO_4]^-$	1 H_2O	$P6_122$ ($P6_522$)	10.480	10.480	15.089	1435	21
none	$[Fe^{III}(H_2O)_2B(PO_4)_2]$	1 H_2O	$P6_522$	9.458	9.458	15.707	1217	22
H_3DETA^{3+}	$[Mn^{II}(H_2O)_2Ga(PO_4)_2]_3^{3-}$	none	$C222_1$	10.039	17.389	16.736	2921	this work, **1**
H_3DETA^{3+}	$[Mn^{II}Ga(PO_4)_2]_3^{3-}$	none	$C222_1$	10.039	17.401	16.503	2883	**1** (dehydrated)

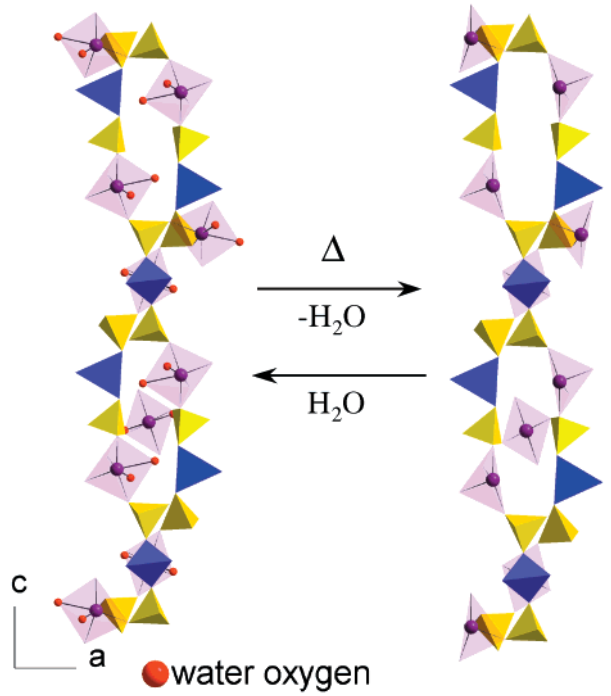

Figure 5. Dehydration−rehydration scheme showing the change of coordination geometry at the Mn sites. The helices shown are $Mn(H_2O)_2Ga(PO_4)_2$ (left) and $MnGa(PO_4)_2$ (right).

MGaPOs. The asymmetric unit contains one tetrahedral M site (where Zn and Ga atoms disorder in a 3:1 ratio), one P, and four O_p atom sites (Figure 2). All are in general positions. Each of the MO_4 tetrahedra shares four common vertexes with four PO_4 tetrahedra to form MPO_4 helices, which in turn interconnect into a UCSB-7 structure type.[28] In contrast to the UCSB-7 series, the framework of **2** can be refined better in the higher symmetry space group $I4_132$ instead of $I2_13$. The T−O−T angles (T = tetrahedral center) are also larger than those found in the UCSB-7 compounds (124°−131° vs 122°−127°). As compared with **1**, the H_3DETA^{3+} cations are much more disordered and they could not be located even when the space symmetry is lowered. Moreover, the transition-metal sites are indistinguishable from that of gallium in **2**. The M−O bond length is between that of Ga−O and Zn−O bonds. Both the structure refinements and chemical analysis confirmed the Zn-to-Ga ratio to be 3:1. An estimation of the porosity of the structure by PLATON analysis[29] reveals that the potential solvent accessible volume for **2** is 34% and that for **1** is 17%, indicating the triple-charged DETA molecules are less bound in **2** and easier to be removed upon heating. This is in accordance with the results of TG analyses, which showed the start-up temperature for the release of organic content is ≈220 °C for **2** and that over 300 °C for **1**.

In conclusion, the first chiral structures in the MGaPO system have been synthesized under mild hydro-

(25) Cowley, A. R.; Chippindale, A. M. *Microporous Mesoporous Mater.* **1999**, *28*, 163.
(26) Logar, N. Z.; Mrak, M.; Kauèiè, V. *J. Solid State Chem.* **2001**, *156*, 480.
(27) Chippindale, A. M.; Cowley, A. R.; Walton, R. I. *J. Mater. Chem.* **1996**, *6*, 611.
(28) Gier, T. E.; Bu, X.; Feng P.; Stucky, G. D. *Nature* **1998**, *395*, 154.
(29) Spek, L. *Acta Crystallogr., Sect. A* **1990**, *46*, C34.

thermal conditions with an achiral triamine as the structure-directing agent. This work has demonstrated that the DETA molecule may play an important role in the formation of the chiral frameworks of **1** and **2**. Both can be prepared in pure chiral forms. As noted in our previous work, it would otherwise result in achiral phases by using diamine in the synthesis.[10,11] The structure of **1** contains magnetic centers of which the coordination number may be thermally manipulated from four to six. The reversible dehydration−hydration nature of the coordination water molecules is rather rare and can be an interesting property in application. It is worth noting that via the same hydrothermal route the Mn and Zn atoms can respectively lead to different chiral phases. Further study on other transition metals to pursue more chiral and novel MGaPO structures will proceed.

Acknowledgment. We are grateful to the National Science Council of the Republic of China for support of this work (NSC 90-2113-M-007-028).

Supporting Information Available: Crystallographic data for **1**, **1** (dehydrated), and **2** and figures showing XRD patterns and plots of **1** (PDF). This material is available free of charge via the Internet at http://pubs.acs.org.

CM010421V